4-2015

Subcutaneous Tissue Depth Over Intraosseous Infusion Sites in a Cadaveric Model

Megan Marie Glazier
Grand Valley State University

Subcutaneous Tissue Depth Over Intraosseous Infusion Sites in a Cadaveric Model

Megan Marie Glazier

A Thesis Submitted to the Graduate Faculty of

GRAND VALLEY STATE UNIVERSITY

In

Partial Fulfillment of the Requirements

For the Degree of

Master of Health Science

Biomedical Sciences

April 2015

Acknowledgements

I thank my committee for their guidance with this project, from the planning in the beginning to the advising at the end. Tim Strickler and Patricia Matthews were essential in giving key suggestions on anatomical structures and clinical implications. And, of course, thank you to Chris Reed for his long-term mentorship and assistance with this project and more. Without approval from Jacque Liles, at the Michigan State University Willed Body Program, this project would not have been possible. A wealth of gratitude to Alex Pereida at Michigan State University, College of Human Medicine, for generously donating his time and facility to help me with this thesis. Debra Burg has been fundamental with her guidance and ingenuity to ensure that this thesis excelled in the right direction. A sincere thank you to the staff at the Grand Valley State University Statistical Consulting Center, for their help computing my data. Many thanks to my family and friends for all of their support, encouragement, and love.

Abstract

BACKGROUND: When emergent intravenous access is not available an intraosseous (IO) infusion is performed. To accurately perform an IO infusion, the healthcare provider must precisely palpate and identify the associated anatomical landmark for placement. A thicker layer of subcutaneous tissue over the insertion site can make this process difficult, leading to an increased risk of misplacement. **PURPOSE:** To relate the subcutaneous tissue depth with body mass index (BMI) and percent body fat in order to better understand IO placement sites in relation to these body composition factors. **SUBJECTS:** Male and female unembalmed cadavers (n=22) between the ages of 54-95 years old were provided by the Willed Body Program in association with Michigan State University, College of Human Medicine, in Grand Rapids, MI. **METHODS AND MATERIALS:** Subcutaneous tissue depth was measured by the insertion of a taper gauge into the skin over six IO infusion sites. Five bilateral skinfold measurements per cadaver were taken using a Lange skinfold caliper to obtain body density which was then converted into percent body fat. BMI was calculated from the cadavers height and weight which was supplied by the Willed Body Program. **RESULTS:** Both BMI and percent body fat demonstrated positive correlations with subcutaneous tissue depth at all sites. Using the Wilcoxon Signed Rank Test, it was observed that embalmed cadavers had significantly larger subcutaneous tissue depth at all sites ($p = 0.0313$) except the distal radius ($p = 0.0625$). **CONCLUSIONS:** This study demonstrated that an increase of subcutaneous tissue depth correlates with increased BMI and percent body fat. When assessing where to place an IO infusion, sites with the least amount of subcutaneous tissue should be considered first, with consideration of injuries and contraindications.

Table of Contents

List of Tables

List of Figures

Introduction

In an emergency setting, it is important to be able to quickly and safely deliver life-saving fluids and medications to the patient. This is achieved by introducing a peripheral intravenous (IV) catheter into one of the patient's peripheral veins. The average time for a peripheral IV line to be placed is 4.4 ± 2.8 minutes, which is insufficient in an extreme emergency setting (Minville et al. 2006). Increased time to place a peripheral IV line can occur when veins are too fragile, narrow, collapsed, or when the patient is an infant, combative or obese. When vascular access is needed immediately, and a peripheral IV line cannot be obtained in a timely manner, healthcare professionals turn to other available options to gain venous access, such as subcutaneous, intramuscular or endotracheal routes (Orlowski 1994). These routes provide quick access for medications to be given to the patient, but with increased difficulty in giving large amounts of fluids and certain medications to the patient in a short amount of time. When these three alternate routes are inappropriate for the treatment needed, a central venous line (CVC) or an intraosseous (IO) infusion is used (Paxton 2012).

An IO infusion is a medical procedure that involves the insertion of a needle into the medullary cavity of bone to gain venous access. As an alternative route for peripheral IV placement, most IO infusions occur in both child and adult patients with small, fragile or collapsed veins, vasoconstriction, burns, or obesity (Paxton 2012; Fowler et al. 2007; Hurran and Dunn 1995). The overall goals when performing an IO infusion are to resuscitate the patient in order to restore organ perfusion and fluid volumes, along with providing life saving medications (Kortbeek et al. 2008; Warren et al. 1993). Current recommendations state that IO placement should be performed when peripheral IV access can not be obtained after three attempts within

two minutes (Deakin et al. 2010; Leidel et al. 2012). IO infusions are primarily used in a pre-hospital setting, such as in ambulance transport or in the emergency department, when venous access is needed immediately (Glaeser et al. 1993; Buck et al. 2007).

Sites for IO placement are determined by ease of access, avoidance of injuries and contraindications, level of obesity, and provider judgment and experience. The most common insertion sites are long bones with anatomical landmarks that are easy to identify and penetrate under a thin layer of skin (Ong et al. 2009). Some of the more common sites for IO placement are the proximal tibia, distal tibia, and proximal humerus (Paxton 2012). Prior to 1998, a medullary cavity was essential for an IO placement site, based on the theory that this was critical for transported materials to reach the general circulation. Since then, the calcaneus and radial styloid process have been shown to properly place and deliver fluids intraosseously as effectively as other IO sites (McCarthy et al. 2003).

Although the frequency of complications from IO infusions is currently low, when they do occur, they can be severe. There are two main categories of complications when performing IO infusions: dislodgment and misplacement. Dislodgments are when the IO needle becomes prematurely removed from the bone in which it was originally inserted. Misplacement of an IO needle is defined as when the needle either over-penetrates or under-penetrates the bone. Under-penetration occurs more frequently, likely due to using an incorrect needle length or excess subcutaneous tissue over the site of insertion (Johnson et al. 2005). Although certain semi-automatic IO devices allow for easier needle selection, under-penetration can still be a problem. Misplacements usually occur because of the inexperience of healthcare providers, incorrect

identification of anatomical landmarks, and excess subcutaneous tissue over the site of insertion (Macnab et al. 2000).

There are many ways to prevent complications from IO infusions, such as longer needle lengths (45 mm) for obese patients, threaded needles, and other mechanisms to secure IO placement (Johnson et al. 2005; Greaves et al. 1999). Even with these safety measures already implemented, misplacements can still occur. Studies have shown that excess subcutaneous tissue over IO insertion sites leads to two problems with IO infusions: inability to correctly identify anatomical landmarks and possible under-penetration, both increasing the risk of misplacements (Leidel et al. 2009; Stouffer et al. 2007; Olsen et al. 2002; Glaeser et al. 1993; Koschel 2005). For the use of IO infusions in obese patients, the healthcare provider must take into account the correct length of needle in order to traverse the skin, subcutaneous tissue, and bone to limit the risk of complications (Fowler et al. 2007; Reades et al. 2011). With obesity as a common condition in those patients for whom IO infusions are necessary, there is a need to know the thickness of the subcutaneous tissue overlying the insertion sites to avoid misplacement of the IO needle (Fowler et al. 2007; Paxton 2012).

Methods

Population

The population of this study consists of cadavers donated to the Willed Body Program of the Michigan State University College of Human Medicine, in Grand Rapids, MI, from June 2014 to February 2015. The Willed Body Program supplied a donor ID number, age at death, height, and weight for all twenty-two individuals. Cadavers were measured prior to embalming within 24 hours of death. The nature of the population gathered represented a sample of

convenience due to the cadavers being donated bodies. Measurements were recorded from fourteen males between the ages of sixty and ninety-five years old, and eight females between the ages of fifty-four and ninety-three years old.

Body Composition

Measurements for skinfold thickness, percent body fat, and body mass index (BMI) were taken on all cadavers. Skinfold thickness was measured bilaterally at five sites (abdomen, chest, suprailiac, thigh, and triceps) using a Lange skinfold caliper according to the methods described by Howely and Thompson (2012). To measure the triceps skinfold site, the corresponding arm was placed at a 90° angle across the chest, so that the palm of the hand was resting on the umbilicus. Then a vertical pinch was made at the midpoint between the acromion process of the scapula and the elbow on the posterior aspect of the brachium.

Figure 1- Right Chest Skinfold Measurement.

The skinfold caliper was placed 10 mm below where the skin was pinched and the triceps site was measured. To obtain the chest skinfold measurement, an oblique pinch was made along the midpoint of the anterior axillary fold between the axilla and the nipple (Figure 1). The skinfold caliper was placed 10 mm medial to where the skin was pinched and this site was measured.

In order to measure skinfold thickness on the abdomen, a vertical pinch was made 5 cm directly lateral to the umbilicus. The skinfold caliper was placed 10 mm below this site and measured. To obtain the suprailiac skinfold measurement, the iliac crest was palpated and a

horizontal pinch was made directly above the iliac crest (Figure 2). The skinfold caliper was then placed 10 mm lateral to this site and the measurement was obtained. In order to measure skinfold thickness on the thigh, the knee was slightly bent and a rolled towel was placed beneath it. A vertical pinch of the skin was made at the center point between the inguinal ligament and the patella, in the middle of the thigh. The skinfold caliper was placed 10 mm below where the skin was pinched and the thigh site was measured.

Figure 2- Right Suprailiac Skinfold Measurement.

From obtained skinfold measurements body density was calculated using the Jackson and Pollock 3-site equations for males and females, respectively (Table 1). Using the calculated body density for each cadaver, percent body fat was determined using the Brožek equation (Table 2).

Male Body Density =	1.10938 - (0.0008267 x sum of chest, abdomen, and thigh skinfolds in mm) + (0.0000016 x square of the sum of chest, abdomen, and thigh skinfolds in mm) - (0.0002574 x age)
Female Body Density =	1.0994921 - (0.0009929 x sum of triceps, thigh, and suprailiac skinfolds in mm) + (0.0000023 x square of the sum of triceps, thigh, and suprailiac skinfolds in mm) - (0.0001392 x age)

Table 1- Jackson and Pollock Equations. Used for body density calculations using the 3-site method (Jackson and Pollock 1978; Jackson et al. 1980).

Percent Fat =	[(457/Body Density) - 414.2]

Table 2- Brožek Equation. Used for calculating percent body fat from body density (Brožek et al. 1963).

Body height and weight was supplied by the funeral home or hospital through the Willed Body Program. BMI was calculated using the formula (Table 3) provided by the Centers for

BMI =	[weight (lb) / [height (in)]^2] x 703

Table 3- Equation for BMI Calculation. (CDC 2015).

Disease Control and Prevention (CDC 2015). The calculated BMI was interpreted and each cadaver was categorized via the standard weight categories (Table 4).

Weight Category	BMI
Underweight	< 18.5
Normal	18.5 - 24.9
Overweight	25.0 - 29.9
Obese	≥ 30

Table 4- Standard Weight Categories. Used to categorize BMI (CDC 2015).

Subcutaneous Depth

Subcutaneous depth was measured bilaterally at five sites (proximal humerus, distal radius, proximal tibia, distal tibia, and calcaneus) and in the midline of the chest (sternum) using a Shinwa measuring taper gauge. The taper gauge was inserted into the cadaver following needle insertion procedures for the previously stated sites of IO infusions, which are established elsewhere (Paxton 2012; Tarrow et al. 1952; McCarthy et al. 2003; Clem and Teirney 2004). In one male, the subcutaneous depth on the left proximal tibia was not measured due to an IO cannula being placed antemortem.

To measure the subcutaneous tissue depth of the sternum, the manubrium was palpated to locate the sternal notch. As illustrated (Figure 3), the taper gauge was inserted at a 90° angle to the bone surface, 15 mm below the sternal notch in the midline of the manubrium (Tarrow et al. 1952). The subcutaneous tissue depth at the proximal humerus was measured by placing the

Figure 3- Subcutaneous Tissue Depth of Sternum.

brachium directly along the trunk and placing the antibrachium at a 90° angle so the palm of the hand was resting on the umbilicus. The greater tubercle of the proximal humerus was palpated and the taper gauge was inserted at a 90° angle to the bone surface, directly on the greater tubercle of the humerus (Paxton 2012). The antibrachium was then placed along the trunk and the shoulder was slightly externally rotated to allow for the lateral radius to face anteriorly. The distal radius was palpated to locate the radial styloid process. Insertion of the taper gauge occurred at a 45° angle, 3 cm proximal to the radial styloid process (McCarthy et al. 2002).

A rolled towel was placed under the knee to obtain a slightly flexed position in order to measure the subcutaneous tissue depth of the proximal tibia. The tibial tuberosity was palpated and the taper gauge was inserted at a 90° angle to the bone surface, 2 cm distally and slightly medial to the tibial tuberosity (Dev et al. 2014). The rolled towel was removed and the hip was then externally rotated to allow for the medial malleolus to be positioned anteriorly. The distal tibia was palpated to locate the flat area of bone 2 cm proximal to the medial malleolus (Figure 4). Insertion of the taper gauge occurred at this site, at a 10°-15° angle in relation to the long axis of the tibia (Paxton 2012). The posterior ankle was placed on a block to raise the lower limb for a better view of the calcaneal insertion site. A line from the calcaneal tuberosity to the medial proximal prominence of metatarsal one was imagined. The medial process of the calcaneal tuberosity was palpated, which should be located on the imagined line 2 cm distally from the calcaneal

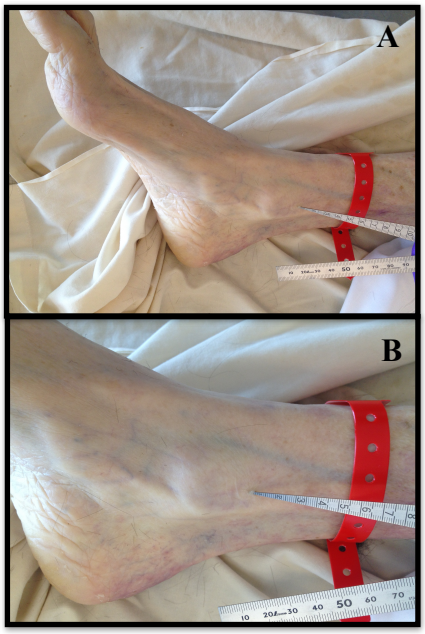

Figure 4- Subcutaneous Tissue Depth Measurement at Distal Tibia (A), and close up (B).

tuberosity. The taper gauge was inserted at a 45° lateral angle at this site (Clem and Tierney 2004).

Results

The twenty-two cadavers were all older adult cadavers, with fourteen males between the ages of sixty and ninety-five years old, and eight females between the ages of fifty-four and ninety-three years old. The range of BMI recorded for males and females was 16.7 to 28.9 and 17.2 to 29.4, respectively. Whereas, percent body fat for males and females ranged from 7.46 to 25.26 and 8.81 to 29.02, respectively (Table 5).

	Male	Female
Number	14	8
Youngest	60	54
Oldest	95	93
Greatest BMI	28.9	29.4
Lowest BMI	16.7	17.2
Greatest % BF	25.26	29.02
Lowest % BF	7.46	8.81

Table 5- Demographic Features of Cadavers.

Correlations were calculated to determine possible relationships between BMI and subcutaneous tissue depth, as well as percent body fat and subcutaneous tissue depth. Both BMI and percent body fat demonstrated a positive correlation with subcutaneous tissue depth at all sites (Table 6). BMI demonstrated a moderate positive relationship at the sternum (0.64691), distal radius (0.66671), proximal tibia (0.66072), and distal tibia (0.57304); and a

	Sternum	Proximal Humerus	Distal Radius	Proximal Tibia	Distal Tibia	Calcaneus
BMI	0.64691	0.36533	0.66671	0.66072	0.57304	0.46301
Percent Body Fat	0.75415	0.64870	0.51380	0.42045	0.51664	0.53762

Table 6- Correlation Data. Correlation of BMI and subcutaneous tissue depth and percent body fat and subcutaneous tissue depth.

mild positive relationship at the proximal humerus (0.36533) and calcaneus (0.46301). All correlations between subcutaneous tissue depth and BMI were significant (sternum p=0.0011, distal radius p=0.0007, proximal tibia p=0.0008, distal tibia p=0.0053 and calcaneus p=0.03) except the proximal humerus (p=0.0946). Percent body fat showed a strong positive relationship at the sternum (0.75415), moderate positive relationships at the proximal humerus (0.64870), distal radius (0.51380), distal tibia (0.51664), and calcaneus (0.53762); and a mild positive relationship at the proximal tibia (0.42045). All correlations between subcutaneous tissue depth and percent body fat were significant (sternum p<0.0001, proximal humerus p=0.0011, distal radius p=0.0144, distal tibia p=0.0138 and calcaneus p=0.0099) except the proximal tibia (p=0.0946).

Six cadavers where measured prior to embalming, as well as after embalming. Using the Wilcoxon Signed Rank Test, it was observed that embalmed cadavers had significantly larger subcutaneous tissue depth at all sites (p=0.0313), except the distal radius (p=0.0625).

Discussion

This study's aim is to determine relationships between BMI and subcutaneous tissue depth, as well as percent body fat and subcutaneous tissue depth, in order to increase knowledge in the field to aid in limiting IO misplacements. Through obtaining skinfold measurements, height, and weight from twenty-two cadavers, BMI and percent body fat was calculated. BMI and percent body fat was then tested against subcutaneous tissue depth that was obtained through taper gauge depth measurements.

All six tested sites show a mild to moderate positive correlation between subcutaneous tissue depth and BMI. The proximal humerus and the calcaneus demonstrated mild positive

correlations between BMI and subcutaneous tissue depth. These sites have a small subcutaneous tissue layer above muscle and thick layers of connective tissue. Furthermore, because BMI cannot distinguish between adipose tissue, muscle, and connective tissue, correlations between BMI and subcutaneous tissue depth at these two sites would not be expected to be strongly positive (Prentice and Jebb 2001). The sternum, distal radius, proximal tibia, and distal tibia showed moderate positive correlation with BMI. Subcutaneous tissue at these sites contain mostly adipose tissue and thin layers of connective tissue, therefore, allowing for a closer correlation between BMI and adipose tissue increase.

Mild, moderate, and strong positive correlations were observed between percent body fat and subcutaneous tissue depth at all tested sites. Subcutaneous tissue depth at the proximal tibia showed a mild positive correlation with percent body fat. Anatomy of the proximal tibia involves a very thin layer of subcutaneous tissue throughout most weight categories. Due to common weight distributions involving mostly the abdomen and femoral/gluteal regions, the overlying subcutaneous tissue layer at the proximal tibia is not particularly thick in non-obese individuals (Feldman et al. 1969). Unlike the proximal tibia, a strong positive correlation was observed between subcutaneous tissue depth at the sternum and percent body fat. The thin layer of subcutaneous tissue that covers the sternum contains mostly adipose tissue and thin layers of connective tissue. Therefore, the increase in adipose tissue in this area will increase the subcutaneous tissue depth while the percent body fat increases as well. The distal radius and distal tibia are similar to the sternum because the subcutaneous tissue overlying these sites contain mostly adipose tissue and thin connective tissue layers. When percent body fat

increases, so does the adipose tissue, leading to a positive correlation between percent body fat and subcutaneous tissue depth.

Embalmed cadavers were shown to have significantly thicker subcutaneous tissue at all sites, except the distal radius, in comparison to unembalmed cadavers. The insignificant difference found between the distal radius of embalmed cadavers and the distal radius of unembalmed cadavers is from the relatively constant thickness of subcutaneous tissue over the site independent of excess fluids. Through the embalming process that is required for cadaver use, in anatomy labs, the subcutaneous tissue layers are filled with embalming fluid to an extent that is different from living individuals. This demonstrated that subcutaneous tissue studies should utilize unembalmed cadavers only, to maintain a close relationship to conditions in living individuals.

Although subcutaneous tissue depth has been widely addressed in forensic studies, craniofacial mapping, and insulin usage, there is a dearth of research pertaining to other aspects of post-cranial subcutaneous tissue depths. This study extends the knowledge of IO infusion placement in relation to BMI, percent body fat, and subcutaneous tissue depth. Future studies should include the use of unembalmed cadavers only, a larger number of cadavers, and more sophisticated anthropometric measuring techniques.

Literature Cited

Brozek J, Grande F, Anderson JT, Keys A. 1963. DENSITOMETRIC ANALYSIS OF BODY COMPOSITION: REVISION OF SOME QUANTITATIVE ASSUMPTIONS. Ann. N. Y. Acad. Sci. 110:113–140.

Buck ML, Wiggins BS, Sesler JM. 2007. Intraosseous Drug Administration in Children and Adults During Cardiopulmonary Resuscitation. Ann Pharmacother 41:1679–1686.

Clem M, Tierney P. 2004. Intraosseous infusions via the calcaneus. Resuscitation 62:107–112.

Deakin CD, Nolan JP, Soar J, Sunde K, Koster RW, Smith GB, Perkins GD. 2010. European Resuscitation Council Guidelines for Resuscitation 2010 Section 4. Adult advanced life support. Resuscitation 81:1305–1352.

Doud EA, Tysell JE. 1942. Massive intramedullary infusions. JAMA 120:1212–1213.

Fowler R, Gallagher JV, Isaacs SM, Ossman E, al et. 2007. The Role of Intraosseous Vascular Access in the Out-of-Hospital Environment (resource Document to Naemsp Position Statement). Prehospital Emergency Care 11:63–6.

Glaeser P, Hellmich T, Szewczuga D, Losek J, Smith D. 1993. Five-Year Experience in Prehospital Intraosseous Infusions in Children and Adults. Annals of Emergency Medicine 22:1119–1124.

Greaves I, Evans GA, Boyle AA. 1999. Intraosseous infusions in the adult. Trauma 1:291–299.

[CDC] Centers for Disease Control and Prevention. Healthy Weight: Assessing Your Weight: BMI: About Adult BMI | DNPAO | CDC. [accessed 2014 Apr 6]. http://www.cdc.gov/healthyweight/assessing/bmi/adult_bmi/index.html#Interpreted

Howley E, Thompson D. 2012. Fitness Professional's Handbook-6th Edition.

Hurren JS, Dunn KW. 1995. Intraosseous infusion for burns resuscitation. Burns 21:285–287.

Jackson AS, Pollock ML. 1978. Generalized equations for predicting body density of men. Br. J. Nutr. 40:497–504.

Jackson AS, Pollock ML, Ward A. 1980. Generalized equations for predicting body density of women. Med Sci Sports Exerc 12:175–181.

Johnson DL, Findlay J, Macnab AJ, Susak L. 2005. Cadaver Testing to Validate Design Criteria of an Adult Intraosseous Infusion System. Military Medicine 170:251–7.

Kortbeek JB, Al Turki SA, Ali J, Antoine JA, Bouillon B, Brasel K, Brenneman F, Brink PR, Brohi K, Burris D, et al. 2008. Advanced trauma life support, 8th edition, the evidence for change. J Trauma 64:1638–1650.

Koschel MJM. 2005. Sternal Intraosseous Infusions: Emergency vascular access in adults. Journal of Nursing January 2005 105:66–68.

Leidel BA, Kirchhoff C, Bogner V, Braunstein V, Biberthaler P, Kanz K-G. 2012. Comparison of intraosseous versus central venous vascular access in adults under resuscitation in the emergency department with inaccessible peripheral veins. Resuscitation 83:40–45.

Leidel BA, Kirchhoff C, Bogner V, Stegmaier J, Mutschler W, Kanz K-G, Braunstein V. 2009. Is the intraosseous access route fast and efficacious compared to conventional central venous catheterization in adult patients under resuscitation in the emergency department? A prospective observational pilot study. Patient Safety in Surgery 3:24.

Macnab A, Christenson J, Findlay J, Horwood B, Johnson D, Jones L, Phillips K, Pollack C, Robinson D, Rumball C, et al. 2000. A New System for Sternal Intraosseous Infusion in Adults. Prehospital Emergency Care 4:173–177.

McCarthy G, O'Donnell C, O'Brien M. 2003. Successful intraosseous infusion in the critically ill patient does not require a medullary cavity. Resuscitation 56:183–186.

Minville V, Pianezza A, Asehnoune K, Cabardis S, Smail N. 2006. Prehospital intravenous line placement assessment in the French emergency system: a prospective study. European Journal of Anaesthesiology 23:594–597.

Olsen D, Packer BE, Perrett J, Balentine H, Andrews GA. 2002. Evaluation of the Bone Injection Gun as a Method for Intraosseous Cannula Placement for Fluid Therapy in Adult Dogs. Veterinary Surgery 31:533–540.

Ong MEH, Chan YH, Oh JJ, Ngo AS-Y. 2009. An observational, prospective study comparing tibial and humeral intraosseous access using the EZ-IO. The American Journal of Emergency Medicine 27:8–15.

Orlowski JP. 1994. Emergency alternatives to intravenous access. Intraosseous, intratracheal, sublingual, and other-site drug administration. Pediatr. Clin. North Am. 41:1183–1199.

Paxton JH. 2012. Intraosseous vascular access: A review. Trauma 14:195–232.

Reades R, Studnek J R, Garrett J S, Vandeventer S, Blackwell T. 2011. Comparison of first-attempt success between tibial and humeral intraosseous insertions during out-of-hospital cardiac arrest. Prehospital Emergency Care 15:278–281.

Stouffer J, Jui J, Acebo J, Hawks R. 2007. The Portlant IO Experience: Results of an Adult Intraosseous Infusion Protocol. Journal of Emergency Medical Services 32:27–28.

Tarrow CAB, Turkel H, Thompson CMS. 1952. INFUSIONS VIA THE BONE MARROW AND BIOPSY OF THE BONE AND BONE MARROW. Anesthesiology 13:501–509–501–509.

Warren D, Kissoon N, Sommerauer J, Rieder M. 1993. Comparison of Fluid Infusion Rates Among Peripheral Intravenous and Humerus, Femur, Malleolus, and Tibial Intraosseous Sites in Normovolemic and Hypovolemic Piglets. Annals of Emergency Medicine 22:183–186.

Introduction

In an emergency setting, it is important to be able to quickly and safely deliver life-saving fluids and medications to the patient. This is usually achieved by introducing a peripheral intravenous (IV) catheter into one of the patient's peripheral veins. The average time for a peripheral IV line to be placed is 4.4 ± 2.8 minutes, which is insufficient in an extreme emergency setting (Minville et al. 2006). Increased time to place a peripheral IV line can occur when veins are too fragile, narrow, collapsed, or when the patient is an infant, combative or obese. When vascular access is needed immediately, and a peripheral IV line cannot be obtained in a timely manner, healthcare professionals turn to other options to gain venous access. Current alternatives to peripheral IV cannulation include subcutaneous, intramuscular or endotracheal routes (Orlowski 1994). These routes provide quick access for medications to be given to the patient, but present difficulty in giving large amounts of fluids and certain medications to the patient in a short amount of time. When these three routes are inappropriate for the treatment needed, a central venous catheter (CVC) or an intraosseous (IO) infusion is used (Paxton 2012).

CVC and IO infusions are more invasive than other routes for peripheral IV cannulation. The advantage of using these routes is that they allow for large amounts of fluids and medications to reach the general circulation, at rates similar to peripheral IVs (Fowler et al. 2007). The use of a CVC is more common in a hospital setting such as the emergency department than in pre-hospital settings due to its complex nature. Along with the complexity of performing a CVC, there are many complications associated with CVC placement that are not associated with IO infusions (Knuth et al. [date unknown]). Therefore, in many emergencies, healthcare professionals will choose to perform IO infusions rather than CVC.

An IO infusion is a medical procedure that involves the insertion of a needle into the medullary cavity of a bone to gain venous access. As an alternative to peripheral IV placement, IO infusions are performed on both child and adult patients which present with small, fragile or collapsed veins, vasoconstriction, burns or obesity (Paxton 2012; Fowler et al. 2007; Hurran and Dunn 1995). IO infusions are used to resuscitate the patient by restoring organ perfusion and fluid volumes, along with providing a route for life saving medications (Kortbeek et al. 2008; Warren et al. 1993). Current recommendations state that IO placement should be performed when peripheral IV access can not be obtained after three attempts within two minutes (Deakin et al. 2010; Leidel et al. 2012). IO infusions are primarily used in a pre-hospital setting, such as at an emergency scene or in ambulance transport, or in the hospital's emergency department when venous access in needed immediately (Glaeser et al. 1993; Buck et al. 2007).

History

In the early 20th century, venous access to the circulatory system was a significant clinical focus (Drinker et al. 1922; Paxton 2012). Drinker et al. (1922) first demonstrated that venous access can be obtained through tibial intraosseous cannulation directly into the medullary cavity of a mammalian bone for therapeutic purposes. By accessing the venous system of the medullary cavity, fluids were introduced to the general circulatory system. In 1933, Josefson (1934) demonstrated the use of IO cannulation in humans. He performed multiple sternal IO cannulations to provide treatment for pernicious anemia and other illnesses. This study influenced others to pursue research in IO placement and its function (Paxton 2012).

Within two decades of the initial IO demonstration, Tocantins and O'Neil (1940) conducted a study with human subjects for sternal and proximal tibial IO placement and

demonstrated that flow rates were similar to that of intravenous cannulation (Tocantins 1940). Following early research by Tocantins (1940) and others (Benda et al. 1940; Doud and Tysell 1942), IO cannulation research and practice increased. During this time, the most common route to obtain venous access was to introduce a metal trocar into the peripheral vein of the patient. Because peripheral IV placement was quite difficult and more dangerous than it is today, IO placement became popular within clinical environments (Paxton 2012).

In the early days of IO research, the sternum was a common IO site in both clinical and research settings. This site was common because of the major working theory that a functional IO must involve the use of red bone marrow due to its hematopoietic abilities (Tocantins and O'Neil 1945). This was countered by research demonstrating that tibial IO placement would be safer and allow for more adequate flow and placement in infants and children (Behr 1944). Sternal IO usage was introduced and recommended prior to peripheral IV attempts in the military in 1944, and continued as a route of choice throughout the remainder of World War II (Bailey 1944).

IO cannulation in adults decreased through the late 1940s, but not for children; and due to the development of plastic disposable catheters, the use of IO infusions decreased further in the 1950s (Rivera et al. 2005). Plastic disposable catheters for peripheral IV, subcutaneous, and endotracheal placement made these routes safer and easier to perform, leading to peripheral IV routes becoming the most common (Rivera et al. 2005). Throughout the 1980s, IO research increased with multiple case studies advocating the importance of IO options for resuscitation in children (Orlowski 1984; Berg 1984). Ultimately, the American Heart Associate, in 1985,

recommended the use of IO infusions as an alternative to peripheral IV cannulation in children (JAMA 1986).

In the 1990s, IO infusions began a resurgence in the pre-hospital and medical settings for adults (Paxton 2012). Rather than using manual needles to penetrate the thick cortical layer of bones in adults, semi-automatic devices were developed. These devices made it easier to reach the bone marrow through the thick cortical layer of bone found at the IO insertion sites in adults. These devices not only helped increase IO cannulation usage in adults, but also enhanced IO cannulation in children (Paxton 2012).

In 2000, the American Heart Association recommended that IO infusions be considered for the first attempt at venous access in children experiencing cardiac arrest (AHA 2000). In the mid-2000s, Pediatric Advanced Life Support, Advanced Cardiac Life Support, and the American Heart Association, approved the use of IO cannulation when peripheral IV access couldn't be obtained in the appropriate timeframe, and for patients in cardiac arrest, IO cannulations should be performed immediately (AHA 2006; Kleinman et al. 2010).

Anatomy of Bones

There are three main portions of adult long bones, the epiphyses, metaphyses, and diaphysis. The epiphysis is a secondary center (or centers) of ossification located on both the proximal and distal ends of the long bones and at sites of major processes for muscular attachment. On the surface of the articulating region of the epiphysis lies articular cartilage that allows for smooth movement within the joint. The diaphysis is a long slim shaft of compact bone which contains a medullary cavity in the central inner space. The flared region between the

diaphysis and the epiphysis, on both the proximal and distal portions is the metaphysis, the region formerly occupied by the growth plate (Standring 2008).

Both compact and cancellous bone matrices are produced in layers and are classified as lamellar bone. The first layer of bone is a connective tissue layer called the periosteum, which is located above multiple layers of calcified bone, and covers all external surfaces of bone where there is no articular cartilage. The periosteum protects the underlying bony tissue, anchors blood vessels and nerves, and participates in the attachment of tendons and ligaments to the bone. Deep to the periosteum lie circumferential lamellae — densely packed compact bone — that encompass the entire bone. Located below the circumferential lamellae are osteons, which are cylindrical structures that make up the majority of compact bone (Standring 2008).

Each osteon consists of concentric lamellae — compact bone layers that surround the central canal. Osteons run parallel to the long axis of the bone and have a central canal known as the Haversian canal. Connecting the Haversian canals perpendicularly are Volkmann's canals. Blood vessels and nerves run through both the Haversian canals and Volkmann's canals allowing communication across the bone. On the endosteal surface of compact bone is a layer of cancellous bone, organized into spicules composed of parallel lamellae (Standring 2008). An inner layer of connective tissue, the endosteum, lines the internal surfaces of bone, such as the medullary cavity and trabeculae.

The medullary cavity of long bones contains blood vessels, as well as bone marrow. Bone marrow is found within the medullary cavity and spaces between the trabeculae of cancellous bone. There are two types of bone marrow: red marrow and yellow marrow. Red bone marrow is a type of hematopoietic tissue and is found between the trabeculae within the

epiphysis of long bones in children. At birth the fetal skeleton contains only red bone marrow, whereas in adulthood, only flat bones of the skull, ribs, sternum, and vertebrae still contain red bone marrow. Red bone marrow decreases throughout aging because it begins to transform into yellow bone marrow during early adolescence. Yellow bone marrow is composed primarily of adipose tissue and is found within the diaphysis of long bones in adults (Hall 2012).

Vasculature of Bone

Blood flow in bones follows two pathways. The first is centrifugal, within the compact bone of the diaphysis, and the second is centripetal, on the outer surface of the bone. There are one or two nutrient arteries that enter the nutrient foramen and follow into the nutrient canal, which lies in the middle-third of the diaphysis. Once the nutrient artery passes through the nutrient canal, it branches into ascending and descending medullary arteries in the medulla. As these arteries further divide into smaller vessels they approach the proximal and distal epiphyses (Laroche 2002). The branches of these vessels anastomose with the branches of the metaphyseal and epiphyseal arteries. Metaphyseal arteries arise from surrounding systemic vessels, whereas epiphyseal arteries are said to come from periarticular vascular arcades (Standring 2008). At the epiphyses, many small veins exit the bone through vascular foramina.

Within the medulla, the ascending and descending branches divide into centripetal branches that stay within the medullary cavity and cortical branches that travel within the cortical bone. The centripetal branches divide into arterioles, then capillaries, and further into medullary sinusoids shaped in hexagonal networks (Standring 2008). These sinusoids drain into a central venous sinus located within the center of the medullary cavity. Within the medullary cavity the central venous sinus branches into veins that follow the path of the ascending, descending, and

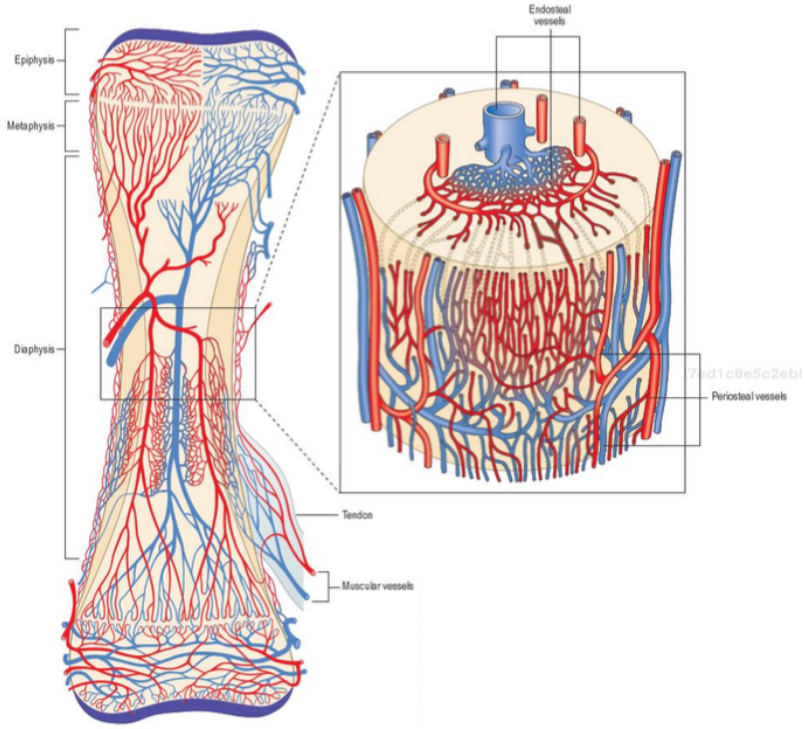

Figure 5- Vasculature of a Long Bone. (Standring 2008).

nutrient arteries (Figure 5). These veins exit the bone with the nutrient artery (nutrient vein) or unaccompanied as emissary veins.

Cortical branches lead to fenestrated cortical capillaries that traverse the Haversian and Volkmann's canals. Volkman canals connect to the medullary cavity for drainage (Laroche 2002). Upon reaching the outer surface of the bone, the cortical capillaries anastomose with periosteal plexuses. Periosteal vessels anastomose with neighboring muscular vessels, allowing a portion of venous drainage to occur by muscular vessels (Standring 2008).

The epiphyseal arteries (nutrient arteries) enter the epiphysis and divide into many small branches that anastomose within the spaces between trabeculae. These vessels eventually drain into epiphyseal sinusoids, that further drain into veins which leave the bone (Laroche 2002).

Vasculature of flat bones differs from that of long bones by primarily being supplied by periosteal vessels (Laroche 2002). These vessels can still drain into a central vein that runs in the trabecular spaces within the center of the bone. The main difference between vasculature of mature and immature bones is that the epiphyses of immature bones have a separate blood supply for the metaphysis and diaphysis, because blood vessels are unable to cross the cartilaginous growth plate (Standring 2008).

Intraosseous Devices and Techniques

Recent advances in medical equipment and techniques have allowed IO infusions to become more common among adults. New devices have made it easier to penetrate through the thick cortical layer of bone, in order to reach the medullary cavity (Weiser et al. 2012). Prior to the approval of semi-automatic IO delivery devices, IO needles where introduced into the bone manually with the Jamshidi™ IO needle or the Cook™ IO needle (Figure 6). The technique for the manual introduction is as follows: once the infusion site is identified and palpated, it should be cleansed by wiping it down with an iodine solution prior to IO insertion. If time allows, an injection of lidocaine, a local anesthetic, can be injected into the skin and subcutaneous tissue overlying the site of insertion. While holding the manual IO needle with the base in the palm of the hand, start to insert the IO needle into the skin. Upon reaching the bone, the index finger and thumb are positioned close to the skin and a twisting motion is used with constant pressure to bore through the bone cortex. Once the medullary cavity is reached, there will be a loss of tension, notifying the provider that the needle has reached the cavity. Manual

Figure 6- Cook™ Manual IO Needle. (Cook-manual-needle.jpg [date unknown]).

insertion, such as this, occurred at all known sites for IO infusion prior to the development of semi-automatic devices (Dev et al. 2014).

In the 1990s, semi-automatic devices made inserting IO catheters into adults faster, more effective and safer. An IO insertion with an automatic or battery powered device can generally be accomplished within one minute and is more accurate than the manual technique (Day 2011). There are several systems that are approved by the Food and Drug Administration, with some of the more popular ones being the EZ-IO®, BIG® (Big Injection Gun), and sternal FAST1® (First Access for Shock and Trauma 1). See Appendix A for more details on semi-automatic devices.

Landmark Identification

Correct landmark identification is particularly important when providing any medical care, especially IO infusions. Several studies demonstrate that the failure to correctly place IO cannulas is caused by either incorrect needle choice or errors in landmark identification (Reades et al. 2011; Paxton et al. 2009; Koschel 2005). Inability to correctly identify anatomical landmarks in children and adults can also be due to inexperienced providers, rare anatomical abnormalities, and excess tissue over the infusion site. Leidel et al. (2009) demonstrated that the main reason for inaccurate IO placement at the proximal humerus was from inability to accurately identify the greater tubercle of the humerus due to excess tissue over the insertion site. Excess tissue can include large muscle mass, an increased adipose layer, or increased body mass index (BMI), making it difficult to accurately palpate bony anatomical structures. Kam and Taylor (2010) demonstrated that an increased BMI strongly correlates with difficulty in accurately performing cannulations in emergency settings. Some dispute exists among past studies on what site is best to use when there is excess tissue over the insertion site. For

example, Paxton et al. (2009) demonstrated that the proximal humerus is an ideal site for obese patients, because of this sites's large anatomical landmark, wheres, Reades et al. (2011a) demonstrated only a 50% success rate using the proximal humerus, due to inability to correctly identify anatomical landmarks.

Intraosseous Infusion Sites

Sites for IO placement are determined by ease of access, avoidance of injuries and contraindications, level of obesity, and provider judgment and experience. The most common insertion sites are long bones with anatomical landmarks that are easy to identify and penetrate under a thin layer of skin at the IO site (Ong et al. 2009). Ultimately, the IO placement site is up to the judgment of the provider and their comfort level. Some of the more common sites for IO infusion are the proximal tibia, distal tibia, and proximal humerus (Paxton 2012).

Proximal Tibia

The proximal tibia is the most common site for intraosseous infusions in both adults and children because it is far away from the site of resuscitation and airway management. In addition the anatomical landmark (the tibial tuberosity) is usually easy to identify due to it being remarkably large, flat, and superficial (Rosenberg and Cheung 2013; Peutrell 2006). When compared to the proximal humerus, the proximal tibia has more successful placements and better flow rates (Reades et al. 2011; Reades et al. 2011a). To properly place an IO infusion on the proximal tibia, the tibial tuberosity must first be located. Then palpate 2 cm distally and slightly medial to find a broad flat area of cortical bone. Needle insertion should occur at a 90º angle to the skin over this anatomical landmark.

Distal Tibia

The distal tibia has similar techniques for accurate IO placement as the proximal tibia. When the proximal tibia cannot be used, the distal tibia is a good alternative due to the thin layer of subcutaneous tissue over the insertion site. The IO placement site for the distal tibia is the medial malleolus. After palpating the medial malleolus move two finger-widths superiorly. This is the correct site for insertion of the needle at an angle of 20-30º in relation to the long axis of the tibia (Day 2011).

Proximal Humerus

The proximal humerus is a common site for IO placement. Paxton et al. (2009) stated that a proximal humerus IO infusion is ideal for obese patients due to the large anatomical landmark this site provides. Other studies have demonstrated that the proximal humerus is a less desirable site than the proximal tibia because it is closer to the site of resuscitation, and it has a smaller, and deeper anatomical landmark to palpate (Reades et al. 2011; Reades et al. 2011a). There are a few different ways to correctly identify the anatomical landmark for IO insertion into the proximal humerus. To start an IO infusion at the proximal humerus, the patient should be in the supine position with the arm at his/her side and elbow bent at a 90º angle with the palm of the hand on the umbillicus. This position increases the prominence of the greater tubercle. Once the greater tubercle is palpated, move one finger-width laterally and insert the IO needle at a 90º angle to the skin. An alternative means of correct anatomical placement starts with the patient in the same position with the healthcare providers' hands placed on the shoulder. The ulnar side of the first hand is placed vertically, just anterior to the axilla and the second hand is placed on the

midline of the lateral humerus. The thumbs then meet in the middle to establish the correct site for IO placement (The Science…2013).

Manubrium

Sternal placement on children has been eschewed since the 1940s, due to the thin bony cortex which increases the risk for complications (Tocantins et al. 1941). Furthermore, because other sites have been found for IO placement, the manubrium has fallen out of clinical use for adults as well. The fact that the sternal location is above and close to the great vessels and vital organs, along with being located near the site of cardiopulmonary resuscitation (CPR) and airway maintenance increases the likelihood of complications. All other common sites for IO placement are located on the extremities and have the benefit of being away from the site of CPR. This leads to a lower risk of fatal complications and a higher frequency of use.

Clavicle

Iwama et al. (1994), have demonstrated that the clavicle can be used as an appropriate alternative to standard IO placement sites. The clavicle is not commonly used clinically for IO placement since placement of an IO cannula here can interfere with CPR delivery.

Ilium

Some earlier studies mention IO infusions in the ilium (Iwama et al. 1994; Tarrow et al. 1952). This site has not been used recently in clinical settings due to the risk of penetration into the pelvic cavity and success rates of other sites.

Distal Femur

The distal femur has been used and is still currently used for IO cannulation in children, though this site is not used in adults (Paxton 2012). The correct site for IO placement on the

anterior distal femur is 2-3 cm proximal to the epicondyles in the midline of the femur (Fiser 1990). Because this site is used only in children, the needle should be angled at 10-30º away from the epiphyseal growth plate to avoid damage (Fiser 1990).

Calcaneus

Prior to 1998, most sites for IO placement were associated with a medullary cavity. It was thought that a cavity was needed for fluids and medication to reach the general circulation. Since then, the calcaneus has been shown as an efficient site to deliver fluids intraosseously just as effectively as the other IO sites in spite of not having a medullary cavity (Clem and Tierney 2004). The calcaneus is an advantageous site for IO placement because it is located far away from the site of resuscitation and it has easy to identify anatomical landmarks. The site for IO placement on the calcaneus is 2 cm from the calcaneal tuberosity toward the medial prominence (Clem and Tierney 2004; McCarthy et al. 2002). The IO needle is then inserted at a 45º angle towards the lateral malleolus.

Distal Radius

The distal aspect of the radius is an appropriate site for IO placement (McCarthy et al. 2002). Waisman and Waisman (1997) demonstrated a 100% success rate when using the distal radius as an IO placement site. Although this data is promising, healthcare personnel are still not regularly using this site for IO infusions. To find the correct site of IO infusion, laterally rotate the arm so that the radius is facing anteriorly when the patient is in the supine position. In this position the base of the radial styloid process of the distal radius is easy to locate for IO insertion.

Complications

Prior to the implementation of semi-automatic devices, complications from IO infusions were more severe and occurred more frequently. Current incidence of complications from IO infusions are low, but when they do occur they can be severe. There are two main sources of complications when performing IO infusions: misplacement and dislodgment. Misplacement of an IO needle is when the needle either over-penetrates or under-penetrates the bone. Under-penetration occurs more frequently, possibly due to using an incorrect needle length or having excess subcutaneous tissue over the site of insertion (Johnson et al. 2005). Although certain semi-automatic IO devices allow for easier needle selection, under-penetration can still be a problem. Misplacements can also occur due to the inexperience of healthcare providers, incorrect identification of anatomical landmarks, and excess subcutaneous tissue over the site of insertion (Macnab et al. 2000). Because obese patients constitute a portion of the population receiving IO infusions, there is a need to be aware of this problem and know the thickness of the subcutaneous tissue overlying the insertion sites (Fowler et al. 2007). This will help to avoid a misplacement of the IO needle.

Dislodgments occur when the IO needle is prematurely removed from the bone in which it was inserted. This can occur during transportation of the patient, especially if the IO needle is not secured properly. Specific complications from dislodgement are more prevalent (roughly 10% of pediatric cases) when using the manual technique of IO placement (Peutrell 2006). Hallas et al. (2013) demonstrated that displacement after insertion occurs 8.5% of the time when using semi-automatic devices. These devices are made to properly insert and secure IO needles. When using the semi-automatic device for sternal IO placement, the safety dome and strain-relief

patch must be dislodged first in order to further dislodge the needle. These extra safety precautions make it extremely difficult to change position of the placed IO catheter, once it is accurately secured (Johnson et al. 2005). Misplacement and dislodgment of IO needles can cause many complications, such as extravasation leading to possible compartment syndrome, subcutaneous abscess, cellulitis, skin infection, osteomyelitis, and necrosis of both muscle and bone (Greaves et al. 1999; Khan et al. 2011).

The most frequent complication of an IO infusion is extravasation, occurring in 3.7% of cases (Hallas et al. 2013; Paxton 2012). Extravasation is the leakage of intraosseous fluids into the surrounding tissues. Leakage can occur from either misplacement or dislodgment of the IO catheter. If extravasation goes unnoticed, it can lead to compartment syndrome (Greaves et al. 1999).

Compartment syndrome has been reported to occur in 0.6% of cases using semi-automatic devices (Hallas et al. 2013). To help lower the risk of compartment syndrome, IO placement should only be attempted at one site per bone, and the IO catheter should be continuously monitored to confirm extravasation is not occurring. An extreme case was depicted in a child by Khan et al. (2011), where both muscle and bone necrosis occurred, along with compartment syndrome. This severe case is the only one reported in recent literature.

Less severe complications, such as subcutaneous abscess and cellulitis, occur in 0.7% of cases (Luck et al. 2010). Osteomyelitis and skin infections occur in 0.4% and 0.3%. respectively (Hallas et al. 2013). Both osteomyelitis and skin infections are thought to be introduced into the body due to failure to correctly clean the injection site prior to insertion. Osteomyelitis seems to

increase in likelihood when the IO catheter remains in the bone for an extended time (Dubick 2000; Greaves et al. 1999).

Sternal IO placement has it its own range of complications. Severe complications include mediastinal abscess, intrapleural infusion, penetration of the great vessels, and death (Greaves et al. 1999). Prior to the semi-automatic device, FAST1®, several of these severe complications from sternal puncture led to death (Bakir 1963).

Contraindications

Though few, there are some contraindications to IO placement. IO infusions should not be placed in bones containing a fracture or through burns or skin infections which overlay the insertion site (Orlowski 1994). Sites used previously for IO placement should also not be used in an effort to lower the risk of extravasation. Patients who have bone or blood diseases, such as osteoporosis, osteogenesis imperfecta, osteopetrosis, septicemia, or acute leukemia, should not have IO infusions (Greaves et al. 1999).

Appendix A: Intraosseous Device Details

The first semi-automatic device on the market was the FAST1® (Fast Access for Shock and Trauma) in 1997, followed by the BIG® (Big Injection Gun) and EZ-IO® in 1998 and 2004 respectively (Paxton 2012). The EZ-IO® is approved for usage in three sites — the proximal and distal tibia and the proximal humerus. This device is battery powered and has three distinct needle lengths, whose use is based on approximate weight. The 15 mm needle is used on individuals between 3-33 kg — usually children. There are two needles intended for use on adults. The first is a 25 mm needle for individuals greater than 40 kg. The second is a 45 mm needle for individuals greater than 40 kg with excess tissue over the site of insertion, and for insertion on the proximal humerus. Healthcare providers need to be able to identify the thickness of subcutaneous tissue to correctly choose which needle to use. Once the ideal insertion site is located, the specific needle choice is attached and the device is placed at a 90º angle to the site. The needle is inserted into the skin until the bone is reached and then inspected to make sure the 5 mm mark (from the base of the needle) is visible. This mark is used to determine if the correct needle was chosen for the corresponding depth of subcutaneous tissue. If the 5 mm mark is not visible, the needle is removed and a larger needle is inserted. Once the correct needle is inserted into the skin, gentle pressure on the power driver is given to insert the needle into the cortex of the bone (EZ-IO [Date Unknown]). Upon reaching the medullary cavity, the provider will feel a release in pressure, indicating that it is time to stop insertion of the device. The power driver and stylet are removed from the insertion site, with the needle being

Figure 7- EZ-IO® device.
(Teleflex Incorporated 2015).

left in place. The catheter is then attached to an intravenous line extension set and secured to the patient via the EZ-Stabilizer™ (The Science…2013).

The BIG® (Big Injection Gun) is only approved for use on the proximal tibia and proximal humerus. This system provides two different devices with associated needles, one for children and one for adults. Once the correct site for insertion is located, the BIG® is placed at a 90º angle to the insertion site. One hand is used to stabilize the BIG® device throughout the entire insertion process. The other hand must release the red safely latch at the top of the device and firmly grasp the sides (referred to as shoulders) of the BIG®. With the shoulders of the BIG® grasped, the palm of that same hand is placed on the top of the device to apply firm pressure to deliver the stylet trocar and needle. After delivery of the stylet trocar and needle, the stylet trocar is removed, and the needle is secured by the safety latch and tape (Adult… 2008).

Figure 8- BIG® Device. (Waismed Ltd. 2009).

Though rarely performed, sternal IO insertions are performed using the FAST1® (First Access for Shock and Trauma 1) system, which is only approved for usage at the manubrium. The FAST1® includes the delivery device, target patch, and dome. The sternal target patch is applied to the cleansed manubrium, identifying the correct location to place the stabilizer points which are located on the FAST1® delivery device. When the delivery device is positioned at a 90º angle to the manubrium, manual pressure is applied, which inserts the stabilizer points into the skin and delivers the IO catheter

Figure 9- FAST1® Device. (05137PA.jpeg [date unknown]).

into the manubrium (Frascone et al. 2007). This device only has one depth setting for IO catheter placement, which eliminates the risk of over-penetration. Upon removal of the delivery device, the catheter is attached to tubing on the target patch. The dome is then attached to cover the target patch so the IO catheter is adequately secured.

Once the IO catheter is placed it should be tested for functionality. Proper placement of the IO needle, fluid flushing, and sometimes, bone marrow aspiration is performed. If proper placement cannot be verified, the device is removed and another site is used for the placement of the IO catheter. Upon confirmation of correct catheter placement, the IO catheter is ready to start introducing fluids and medications to the patient.

Appendix B: Body Composition Details

Skinfold measurements, BMI, and percent body fat are used to delineate obese and non-obese individuals (Sardinha et al. 1999; Wellens et al. 1996). Skinfold measurements are commonly used in both clinical and research settings as a way to quantify the subcutaneous adipose layer and the level of total body fat (Deurenberg et al. 2009; Heymsfield et al. 2000). This technique is noninvasive, easy to perform, and inexpensive. While taking skinfold measurements, factors such as age, sex, and site, need to be taken into consideration (Heymsfield et al. 2005). Understanding these factors are important to the overall outcome of measurements. Thus, many studies have provided a basic understanding for expected skinfold measurements depending on age, sex, race, and level of obesity (Gallagher et al. 2000). To help lessen the bias of a single site measurement on the overall outcome of skinfold measurements, it is best to perform measurements at multiple sites per patient.

Through skinfold measurements, researchers are able to calculate body density and percent body fat to gain a better perspective of adiposity within an individual. For adults older than sixty years, the ability to calculate body density from obtained skinfold measurement is achieved by using the following Jackson and Pollock 3-site equations for males and females, respectively (Jackson and Pollock 1978; Jackson et al. 1980):

> Male Body Density = 1.10938 - (0.0008267 x sum of chest, abdomen, and thigh skinfolds in mm) + (0,0000016 x square of the sum of chest, abdomen, and thigh skinfolds in mm) - (0.0002574 x age)

Female Body Density = 1.0994921 - (0.0009929 x sum of triceps, thigh, and suprailiac skinfolds in mm) + (0.0000023 x square of the sum of triceps, thigh, and suprailiac skinfolds in mm) - (0.0001392 x age)

Once body density is calculated, it is used to determine percent body fat. Many studies use the Brožek equation to convert body density to percent body fat. The Brožek equation is (Brožek et al. 1963):

Percent Body Fat = [(457/body density) - 414.2]

This equation has been shown to overestimate the percent body fat in older individuals when compared to DEXA — dual energy x-ray absorptiometry (Guerra et al. 2009). This over-representation needs to be considered when using skinfold measurements and the Brožek equation to obtain percent body fat, particularly when DEXA is not available.

In older individuals, the measurement of body fat is considered an important assessment of the individual's overall health. This can be measured by calculating BMI and percent body fat. BMI is used to categorize individuals as underweight, normal weight, overweight, or obese, whereas, percent body fat is used to determine the amount of overall weight which is due to fat. There are some concerns when using BMI to obtain percent body fat in older individuals due to changes in the skin, adipose patterning, and loss of skeletal muscle and bone (Heymsfield et al. 2005). These changes can cause misinterpretation of data when obtaining BMI for calculating percent body fat. Gallagher et al. (2000) described an overall idea of the relationship between BMI ranges and percent body fat in Caucasian adults in ages ranging from 40-59 and 60-79. He

showed that within the same BMI range there is an increase in percent body fat with an increase in age. There is still a lack of research on elderly individuals and the relationship between BMI and percent body fat.

Appendix C: Data Retrieval Tables

A) Example of Unembalmed Data Retrieval Table

Donor ID: 4315			**Age- 60**	**Sex- M**
			Height- 6'0"	**Weight- 140**
			BMI- 19.0	
			Level Obesity- Normal	
Skinfold	**Unembalmed**			
Chest	8	8		
Abdomen	5	3		
Supriliac	5	5		
Thigh	5	5		
Triceps	4	4		
Sites	**R**	**L**		
Sternum	5			
Proximal Humerus	10	10		
Distal Radius	5	4		
Proximal Tibia	5	5		
Distal Tibia	3	4		
Calcaneus	15	14		
Notes				

B) Example of Unembalmed and Embalmed Data Retrieval Table

Donor ID: 4305			**Age- 90**	**Sex- F**
			Height- 5’2"	**Weight- 125**
			BMI- 22.9	
			Level Obesity- Normal	
Skinfold	**Unembalmed**			
Chest	3	3		
Abdomen	2	3		
Supriliac	2	3		
Thigh	10	13		
Triceps	4	4		
			Embalmed	
Sites	**R**	**L**	**R**	**L**
Sternum	6		7	
Proximal Humerus	11	11	17	18
Distal Radius	7	6	10	10
Proximal Tibia	7	8	12	15
Distal Tibia	3	10	12	22
Calcaneus	13	15	15	28
Notes		L leg swollen		

Appendix D: Statistical Analyses

The SAS System

The CORR Procedure

BMI

1 With Variables:	BMI
6 Variables:	U_Sternum U_RPH U_RDR U_RPT U_RDT U_RC

Simple Statistics BMI

Variable	N	Mean	Std Dev	Sum	Minimum	Maximum	Label
BMI	22	23.2	3.75271	510.4	16.7	29.4	BMI
U_Sternum	22	7.95455	3.33063	175	3	15	U Sternum
U_RPH	22	12.04545	3.94579	265	5	22	U RPH
U_RDR	22	7.5	2.8073	165	3	16	U RDR
U_RPT	22	7.09091	3.72775	156	3	21	U RPT
U_RDT	22	6.18182	2.66613	136	2	12	U RDT
U_RC	22	20.22727	5.9115	445	12	32	U RC

Pearson Correlation Coefficients, N = 22 Prob > |r| under H0: Rho=0

	U_Sternum	U_RPH	U_RDR	U_RPT	U_RDT	U_RC
BMI	0.64691	0.36533	0.66671	0.66072	0.57304	0.46301
BMI	0.0011	0.0946	0.0007	0.0008	0.0053	0.03

The SAS System

The CORR Procedure

Percent Body Fat

1 With Variables:	__Body_Fat
6 Variables:	U_Sternum U_RPH U_RDR U_RPT U_RDT U_RC

Simple Statistics Percent Body Fat

Variable	N	Mean	Std Dev	Sum	Minimum	Maximum	Label
__Body_Fat	22	16.08182	5.94911	353.8	7.46	29.02	% Body Fat
U_Sternum	22	7.95455	3.33063	175	3	15	U Sternum
U_RPH	22	12.04545	3.94579	265	5	22	U RPH
U_RDR	22	7.5	2.8073	165	3	16	U RDR
U_RPT	22	7.09091	3.72775	156	3	21	U RPT
U_RDT	22	6.18182	2.66613	136	2	12	U RDT
U_RC	22	20.22727	5.9115	445	12	32	U RC

Pearson Correlation Coefficients, N = 22, Prob > |r| under H0: Rho=0

	U_Sternum	U_RPH	U_RDR	U_RPT	U_RDT	U_RC
__Body_Fat	0.75415	0.6487	0.5138	0.42045	0.51664	0.53762
% Body Fat	<.0001	0.0011	0.0144	0.0514	0.0138	0.0099

The SAS System

The UNIVARIATE Procedure

Variable: diff_Sternum

Moments Sternum

N	6	Sum Weights	6
Mean	15.5	Sum Observations	93
Std Deviation	15.2019736	Variance	231.1
Skewness	1.04648896	Kurtosis	0.27570622
Uncorrected SS	2597	Corrected SS	1155.5
Coeff Variation	98.0772487	Std Error Mean	6.20617972

Basic Statistical Measures Sternum

Location		Variability	
Mean	15.5	Std Deviation	15.20197
Median	11	Variance	231.1
Mode	.	Range	40
		Interquartile Range	21

Tests for Location: Mu0=0 Sternum

Test	**Statistic**		**p Value**	
Student's t	t	2.497511	Pr > |t|	0.0547
Sign	M	3	Pr >= |M|	0.0313
Signed Rank	S	10.5	Pr >= |S|	0.0313

Quantiles (Definition 5)
Sternum

Level	Quantile
100% Max	41
99%	41
95%	41
90%	41
75% Q3	25
50% Median	11
25% Q1	4
10%	1
5%	1
1%	1
0% Min	1

Extreme Observations
Sternum

Lowest		Highest	
Value	Obs	Value	Obs
1	1	4	2
4	2	7	4
7	4	15	5
15	5	25	6
25	6	41	3

The SAS System

The UNIVARIATE Procedure

Variable: diff_rph

Moments R. Proximal Humerus

N	6	Sum Weights	6
Mean	13.5	Sum Observations	81
Std Deviation	14.1527383	Variance	200.3
Skewness	2.30492982	Kurtosis	5.44179487
Uncorrected SS	2095	Corrected SS	1001.5
Coeff Variation	104.835098	Std Error Mean	5.7778312

Basic Statistical Measures R. Proximal Humerus

Location		**Variability**	
Mean	13.5	Std Deviation	14.15274
Median	8.5	Variance	200.3
Mode	.	Range	37
		Interquartile Range	5

Tests for Location: Mu0=0 R. Proximal Humerus

Test	**Statistic**		**p Value**	
Student's t	t	2.336517	Pr > |t|	0.0667
Sign	M	3	Pr >= |M|	0.0313
Signed Rank	S	10.5	Pr >= |S|	0.0313

Quantiles (Definition 5)
R. Proximal Humerus

Level	Quantile
100% Max	42
99%	42
95%	42
90%	42
75% Q3	11
50% Median	8.5
25% Q1	6
10%	5
5%	5
1%	5
0% Min	5

Extreme Observations
R. Proximal Humerus

Lowest		**Highest**	
Value	Obs	Value	Obs
5	2	6	1
6	1	7	5
7	5	10	4
10	4	11	3
11	3	42	6

The SAS System

The UNIVARIATE Procedure

Variable: diff_rdr

Moments R. Distal Radius

N	6	Sum Weights	6
Mean	2.83333333	Sum Observations	17
Std Deviation	2.31660671	Variance	5.36666667
Skewness	0.30028929	Kurtosis	-1.4177694
Uncorrected SS	75	Corrected SS	26.8333333
Coeff Variation	81.7625899	Std Error Mean	0.94575073

Basic Stastical Measures R. Distal Radius

Location		**Variability**	
Mean	2.833333	Std Deviation	2.31661
Median	2.5	Variance	5.36667
Mode	.	Range	6
		Interquartile Range	4

Tests for Location: Mu0=0 R. Distal Radius

Test	**Statistic**		**p Value**	
Student's t	t	2.995856	Pr > |t|	0.0302
Sign	M	2.5	Pr >= |M|	0.0625
Signed Rank	S	7.5	Pr >= |S|	0.0625

Quantiles (Definition 5)
R. Distal Radius

Level	Quantile
100% Max	6
99%	6
95%	6
90%	6
75% Q3	5
50% Median	2.5
25% Q1	1
10%	0
5%	0
1%	0
0% Min	0

Extrememem Observations
R. Distal Radius

Lowest		**Highest**	
Value	Obs	Value	Obs
0	2	1	5
1	5	2	3
2	3	3	1
3	1	5	6
5	6	6	4

The SAS System

The UNIVARIATE Procedure

Variable: diff_rpt

Moments R. Promixal Tibia

N	6	Sum Weights	6
Mean	8.83333333	Sum Observations	53
Std Deviation	3.97072621	Variance	15.7666667
Skewness	0.32798171	Kurtosis	-0.0226613
Uncorrected SS	547	Corrected SS	78.8333333
Coeff Variation	44.9516175	Std Error Mean	1.62104219

Basic Statistical Measures R. Promixal Tibia

Location		**Variability**	
Mean	8.83333	Std Deviation	3.97073
Median	9.5	Variance	15.76667
Mode	10	Range	11
		Interquartile Range	5

Tests for Location: Mu0=0 R. Promixal Tibia

Test	**Statistic**		**p Value**	
Student's t	t	5.449169	Pr > |t|	0.0028
Sign	M	3	Pr >= |M|	0.0313
Signed Rank	S	10.5	Pr >= |S|	0.0313

Quantiles (Definition 5)
R. Promixal Tibia

Level	Quantile
100% Max	15
99%	15
95%	15
90%	15
75% Q3	10
50% Median	9.5
25% Q1	5
10%	4
5%	4
1%	4
0% Min	4

Extreme Observations
R. Promixal Tibia

Lowest		**Highest**	
Value	Obs	Value	Obs
4	3	5	1
5	1	9	2
9	2	10	4
10	5	10	5
10	4	15	6

The SAS System

The UNIVARIATE Procedure

Variable: diff_rdt

Moments R. Distal Tibia

N	6	Sum Weights	6
Mean	5.66666667	Sum Observations	34
Std Deviation	4.80277697	Variance	23.0666667
Skewness	0.63246165	Kurtosis	-1.1790404
Uncorrected SS	308	Corrected SS	115.333333
Coeff Variation	84.7548878	Std Error Mean	1.96072549

Basic Statistical Measures R. Distal Tibia

Location		**Variability**	
Mean	5.666667	Std Deviation	4.80278
Median	4.5	Variance	23.06667
Mode	2	Range	12
		Interquartile Range	7

Tests for Location: Mu0=0 R. Distal Tibia

Test	**Statistic**		**p Value**	
Student's t	t	2.890087	Pr > |t|	0.0342
Sign	M	3	Pr >= |M|	0.0313
Signed Rank	S	10.5	Pr >= |S|	0.0313

Quantiles (Definition 5)
R. Distal Tibia

Level	Quantile
100% Max	13
99%	13
95%	13
90%	13
75% Q3	9
50% Median	4.5
25% Q1	2
10%	1
5%	1
1%	1
0% Min	1

Extreme Observations
R. Distal Tibia

Lowest		**Highest**	
Value	Obs	Value	Obs
1	4	2	2
2	6	2	6
2	2	7	5
7	5	9	1
9	1	13	3

The SAS System

The UNIVARIATE Procedure

Variable: diff_rc

Moments R. Calcaneus

N	6	Sum Weights	6
Mean	4.5	Sum Observations	27
Std Deviation	3.27108545	Variance	10.7
Skewness	1.23426405	Kurtosis	0.12315486
Uncorrected SS	175	Corrected SS	53.5
Coeff Variation	72.6907877	Std Error Mean	1.33541504

Basic Statistical Measures R. Calcaneus

Location		**Variability**	
Mean	4.5	Std Deviation	3.27109
Median	3	Variance	10.7
Mode	2	Range	8
		Interquartile Range	5
	Note: The mode displayed is the smallest of 2 modes with a count of 2.		

Tests for Location: Mu0=0 R. Calcaneus

Test	**Statistic**		**p Value**	
Student's t	t	3.369739	Pr > |t|	0.0199
Sign	M	3	Pr >= |M|	0.0313
Signed Rank	S	10.5	Pr >= |S|	0.0313

Quantiles (Definition 5)
R. Calcaneus

Level	Quantile
100% Max	10
99%	10
95%	10
90%	10
75% Q3	7
50% Median	3
25% Q1	2
10%	2
5%	2
1%	2
0% Min	2

Extreme Observations
R. Calcaneus

Lowest		**Highest**	
Value	Obs	Value	Obs
2	3	2	3
2	1	3	2
3	4	3	4
3	2	7	5
7	5	10	6

Appendix E: Data Tables

Skinfold	4304	4305	4306	4307	4308
UCR	8	3	4	10	20
UAR	6	2	2	6	16
USR	6	2	7	8	7
UThR	18	10	5	19	18
UTR	7	4	7	11	20
UCL	5	3	4	11	15
UAL	5	3	1	6	20
USL	6	3	5	9	8
UThL	23	13	6	20	16
UTL	5	4	9	13	18
Sites	**4304**	**4305**	**4306**	**4307**	**4308**
U Sternum	4	6	7	8	10
U RPH	11	11	12	8	11
U RDR	5	7	7	8	10
U RPT	4	7	4	21	7
U RDT	5	3	6	6	7
U RC	13	13	15	15	19
U LPH	11	11	15	9	10
U LDR	8	6	8	11	9
U LPT	8	8	8	17	5
U LDT	5	*10	8	7	7
U LC	14	15	14	18	17
Age	**93**	**90**	**91**	**67**	**81**
Sex	**F**	**F**	**F**	**F**	**M**
Height	**5'0"**	**5'2"**	**4'9"**	**4'9"**	**5'0"**
Weight	**105**	**125**	**101**	**136**	**136**
BMI	**20.5**	**22.9**	**21.9**	**29.4**	**26.6**
Body Density	**1.0579569**	**1.0716665**	**1.0687901**	**1.0557567**	**1.0485544**
%Body Fat	**17.76**	**12.24**	**13.39**	**18.66**	**21.64**

Skinfold	4309	4310	4311	4312	4313
UCR	11	30	20	20	12
UAR	15	24	12	12	15
USR	11	20	17	15	8
UThR	16	29	18	20	16
UTR	6	25	25	13	6
UCL	11	24	19	19	12
UAL	16	23	10	11	14
USL	12	20	19	14	7
UThL	17	31	19	21	11
UTL	7	24	19	14	7
Sites	**4309**	**4310**	**4311**	**4312**	**4313**
U Sternum	12	15	8	8	8
U RPH	11	15	13	18	17
U RDR	9	10	16	5	10
U RPT	10	7	10	8	10
U RDT	7	8	9	6	10
U RC	20	26	32	25	22
U LPH	10	18	14	16	17
U LDR	8	10	15	5	8
U LPT	10	8	9	8	10
U LDT	7	7	7	5	7
U LC	19	25	30	23	22
Age	**84**	**54**	**86**	**91**	**95**
Sex	**M**	**F**	**M**	**F**	**M**
Height	**6'0"**	**5'5"**	**5'8"**	**5'4"**	**5'7"**
Weight	**190**	**170**	**190**	**157**	**150**
BMI	**25.8**	**28.3**	**28.9**	**26.9**	**23.5**
Body Density	**1.0558594**	**1.0310955**	**1.0499086**	**1.0444649**	**1.0523373**
% Body Fat	**18.62**	**29.02**	**21.08**	**23.34**	**20.08**

Skinfold	4314	4315	4316	4317	4318
UCR	4	8	15	9	20
UAR	2	5	12	5	15
USR	3	5	8	8	8
UThR	2	5	11	7	10
UTR	3	4	5	9	20
UCL	4	8	12	7	18
UAL	2	3	10	7	15
USL	3	5	9	8	10
UThL	2	5	7	6	12
UTL	4	4	6	7	20
Sites	**4314**	**4315**	**4316**	**4317**	**4318**
U Sternum	3	5	12	5	10
U RPH	8	10	14	10	22
U RDR	3	5	5	4	8
U RPT	3	5	5	6	8
U RDT	2	3	5	3	7
U RC	16	15	17	21	27
U LPH	6	10	12	12	15
U LDR	4	4	6	7	7
U LPT	3	5	4	7	9
U LDT	2	4	2	4	7
U LC	13	14	17	20	25
Age	**74**	**60**	**92**	**85**	**85**
Sex	**M**	**M**	**M**	**M**	**F**
Height	**5'8"**	**6'0"**	**5'9"**	**5'5"**	**5'3"**
Weight	**110**	**140**	**143**	**125**	**134**
BMI	**16.7**	**19.0**	**21.1**	**20.8**	**23.7**
Body Density	**1.0838212**	**1.0795738**	**1.056595**	**1.0708459**	**1.0532511**
% Body Fat	**7.46**	**9.12**	**18.32**	**12.57**	**19.69**

Skinfold	4319	4320	4325	4326	4328
UCR	5	*27	6	3	2
UAR	11	*29	11	5	5
USR	10	17	9	3	2
UThR	9	10	7	5	5
UTR	4	18	5	4	4
UCL	4	*34	4	3	2
UAL	9	*33	11	4	5
USL	10	15	6	3	2
UThL	9	10	7	5	5
UTL	4	11	5	*15	5
Sites	**4319**	**4320**	**4325**	**4326**	**4328**
U Sternum	7	15	3	7	6
U RPH	7	17	12	12	5
U RDR	6	10	7	9	6
U RPT	6	8	7	5	4
U RDT	9	9	12	5	2
U RC	12	31	17	17	20
U LPH	7	16	10	12	6
U LDR	4	9	7	7	6
U LPT	7	9	~ HAS IO ~	7	5
U LDT	5	9	10	3	3
U LC	20	30	17	18	19
Age	**63**	**85**	**78**	**69**	**61**
Sex	**M**	**M**	**M**	**M**	**F**
Height	**5'11"**	**6'3"**	**5'9"**	**5'7"**	**5'4"**
Weight	**174**	**223**	**140**	**129**	**100**
BMI	**24.3**	**27.9**	**20.7**	**20.2**	**17.2**
Body Density	**1.0734963**	**1.0399084**	**1.0703836**	**1.0811427**	**1.0803573**
% Body Fat	**11.51**	**25.26**	**12.75**	**8.50**	**8.81**

Skinfold	4329	4330
UCR	7	7
UAR	11	7
USR	7	8
UThR	6	8
UTR	7	8
UCL	9	8
UAL	13	10
USL	10	6
UThL	10	9
UTL	9	4
Sites	**4329**	**4330**
U Sternum	8	8
U RPH	12	9
U RDR	7	8
U RPT	7	4
U RDT	5	7
U RC	25	27
U LPH	10	11
U LDR	7	6
U LPT	7	5
U LDT	5	7
U LC	26	29
Age	73	74
Sex	M	M
Height	5'8"	5'8"
Weight	130	160
BMI	19.8	24.3
Body Density	10716706	1.0729194
% Body Fat	12.24	11.74

Literature Cited

05137PA.jpg (JPEG Image, 400 × 400 pixels) - Scaled (0%). [accessed 2014 Apr 10]. http://www.chinookmed.com/mas_assets/full/05137PA.jpg

Adult Bone Injection Gun Instructions. 2008. Houston (TX): WaisMed USA. Available from http///www.waismed.com/Documents/Brochures/wwUSA%2015062008.pdf

[AHA] American Heart Association. 2000. Guidelines 2000 for Cardiopulmonary Resuscitation and Emergency Cardiovascular Care. Part 10: Pediatric Advanced Life Support. Circulation 102:I–291–I–342.

[AHA] American Heart Association. 2006. 2005 American Heart Association (AHA) Guidelines for Cardiopulmonary Resuscitation (CPR) and Emergency Cardiovascular Care (ECC) of Pediatric and Neonatal Patients: Pediatric Advanced Life Support. Pediatrics 117:e1005–e1028.

Bailey H. 1944. Bone Marrow as a Site for the Reception of Infusions, Transfusion, and Anaesthetic Agentsa Review of the Present Position. Anesthesiology 5:545–545.

Bailey P. Intraosseous infusion. UpToDate. [accessed 2014 Aug 4]. http://www.uptodate.com/contents/intraosseous-infusion#H6

Bakir F. 1963. Fatal sternal puncture : Report of a case. Chest 44:435–439.

Behr G. 1944. BONE-MARROW INFUSIONS FOR INFANTS. The Lancet 244:472–473.

Berg RA. 1984. Emergency infusion of catecholamines into bone marrow. Am. J. Dis. Child. 138:810–811.

BJORNTORP P. 1991. ADIPOSE-TISSUE DISTRIBUTION AND FUNCTION. INTERNATIONAL JOURNAL OF OBESITY 15:67 – 81.

Brozek J, Grande F, Anderson JT, Keys A. 1963. DENSITOMETRIC ANALYSIS OF BODY COMPOSITION: REVISION OF SOME QUANTITATIVE ASSUMPTIONS. Ann. N. Y. Acad. Sci. 110:113–140.

Buck ML, Wiggins BS, Sesler JM. 2007. Intraosseous Drug Administration in Children and Adults During Cardiopulmonary Resuscitation. Ann Pharmacother 41:1679–1686.

Clem M, Tierney P. 2004. Intraosseous infusions via the calcaneus. Resuscitation 62:107–112.

Cook-manual-needle.jpg (JPEG Image, 300 × 235 pixels) - Scaled (0%). [accessed 2014 Apr 9]. http://ems-praetorian.netdna-ssl.com/Cook-manual-needle.jpg

Day M. 2011. Intraosseous Devices for Intravascular Access in Adult Trauma Patients. American Association of Critical Care Nurses 31:76–90.

Deakin CD, Nolan JP, Soar J, Sunde K, Koster RW, Smith GB, Perkins GD. 2010. European Resuscitation Council Guidelines for Resuscitation 2010 Section 4. Adult advanced life support. Resuscitation 81:1305–1352.

Deurenberg P, Deurenberg-Yap M. 2009. Ageing and changes in body composition: the importance of valid measurements. Woodhead Publishing in Food Science, Technology and Nutrition:169–183.

Dev SP, Stefan RA, Saun T, Lee S. 2014. Insertion of an Intraosseous Needle in Adults. The New England Journal of Medicine 370:e35.

Doud EA, Tysell JE. 1942. Massive intramedullary infusions. JAMA 120:1212–1213.

Drinker C, Drinker K, Lund C. 1922. The Circulation in the Mammalian Bone-Marrow. The American Journal of Physiology 62:1–89.

Dubick MA, Holcomb JB. 2000. A review of intraosseous vascular access: current status and military application. Mil Med 165:552–559.

EZ-IO Product Introductory Program 070807.ppt - EZIO Introduction - for UTMB Website and Training.pdf. [Date unknown]. http://www.utmb.edu/edlab/ezio/TrainingPDFNotes/EZIO%20Introduction%20-%20for%20UTMB%20Website%20and%20Training.pdf

Feldman R, Sender AJ, Siegelaub AB. 1969. Difference in diabetic and nondiabetic fat distribution patterns by skinfold measurements. Diabetes 18:478.

Fiser DH. 1990. Intraosseous infusion. N. Engl. J. Med. 322:1579–1581.

Fowler R, Gallagher JV, Isaacs SM, Ossman E, al et. 2007. The Role of Intraosseous Vascular Access in the Out-of-Hospital Environment (resource Document to Naemsp Position Statement). Prehospital Emergency Care 11:63–6.

Frascone RJ, Jensen JP, Kaye K, Salzman JG. 2007. Consecutive field trials using two different intraosseous devices. Prehosp Emerg Care 11:164–171.

Gallagher D, Heymsfield SB, Heo M, Jebb SA, Murgatroyd PR, Sakamoto Y. 2000. Healthy percentage body fat ranges: an approach for developing guidelines based on body mass index. Am. J. Clin. Nutr. 72:694–701.

Glaeser P, Hellmich T, Szewczuga D, Losek J, Smith D. 1993. Five-Year Experience in Prehospital Intraosseous Infusions in Children and Adults. Annals of Emergency Medicine 22:1119–1124.

Greaves I, Evans GA, Boyle AA. 1999. Intraosseous infusions in the adult. Trauma 1:291–299.

Guerra RS, Amaral TF, Marques E, Mota J, Restivo MT. 2010. Accuracy of Siri and Brozek equations in the percent body fat estimation in older adults. J Nutr Health Aging 14:744–748.

Hall SJ. 2012. Basic biomechanics. 6th ed. New York, NY: McGraw-Hill.

Hallas P, Brabrand M, Folkestad L. 2013. Complication with intraosseous access: scandinavian users' experience. West J Emerg Med 14:440–443.

Healthy Weight: Assessing Your Weight: BMI: About Adult BMI | DNPAO | CDC. [accessed 2014 Apr 6]. http://www.cdc.gov/healthyweight/assessing/bmi/adult_bmi/index.html#Interpreted

Heymsfield S, Lohman T, Wang Z, Going S. 2005. Human Body Composition. 2nd ed. Champaign, IL: Human Kinetics.

Heymsfield SB, Nuñez C, Testolin C, Gallagher D. 2000. Anthropometry and methods of body composition measurement for research and field application in the elderly. Eur J Clin Nutr 54 Suppl 3:S26–32.

Hurren JS, Dunn KW. 1995. Intraosseous infusion for burns resuscitation. Burns 21:285–287.

Iwama H, Katsumi A, Shinohara K, Kawamae K, Ohtomo Y, Akama Y, Tase C, Okuaki A. 1994. Clavicular approach to intraosseous infusion in adults. Fukushima J Med Sci 40:1–8.

Jackson AS, Pollock ML. 1978. Generalized equations for predicting body density of men. Br. J. Nutr. 40:497–504.

Jackson AS, Pollock ML, Ward A. 1980. Generalized equations for predicting body density of women. Med Sci Sports Exerc 12:175–181.

[JAMA] The Journal of the American Medical Association. 1986. Standars and Guidelines for Cardiopulmonary Resuscitation (CPR) and Emergency Cardiac Care (ECC). JAMA 255(21): 2905-2914.

Johnson DL, Findlay J, Macnab AJ, Susak L. 2005. Cadaver Testing to Validate Design Criteria of an Adult Intraosseous Infusion System. Military Medicine 170:251–7.

Josefson A. 1934. A New Method of Treatment- Intraosseous Injections. Acta Medica Scandinavica 81:550–564.

Kam J, Taylor DM. 2010. Obesity significantly increases the difficulty of patient management in the emergency department. Emerg Med Australas 22:316–323.

Khan LAK, Anakwe RE, Murray A, Godwin Y. 2011. A severe complication following intraosseous infusion used during resuscitation of a child. Injury Extra 42:173–177.

Kleinman ME, Chameides L, Schexnayder SM, Samson RA, Hazinski MF, Atkins DL, Berg MD, Caen AR de, Fink EL, Freid EB, et al. 2010. Part 14: Pediatric Advanced Life Support 2010 American Heart Association Guidelines for Cardiopulmonary Resuscitation and Emergency Cardiovascular Care. Circulation 122:S876–S908.

Knuth TE, Beamer C, Davidoff JB, Malik K, Swanson ER. [Date unknown]. Central Venous Lines in Emergencies Time for a New Approach. Vidacare. Avialable from http://www.bc-cesu.ch/pdf/Central_Venous_Lines_in_Emergencies.pdf

Kortbeek JB, Al Turki SA, Ali J, Antoine JA, Bouillon B, Brasel K, Brenneman F, Brink PR, Brohi K, Burris D, et al. 2008. Advanced trauma life support, 8th edition, the evidence for change. J Trauma 64:1638–1650.

Koschel MJM. 2005. Sternal Intraosseous Infusions: Emergency vascular access in adults. Journal of Nursing January 2005 105:66–68.

Laroche M. 2002. Intraosseous circulation from physiology to disease. Joint Bone Spine 69:262–269.

Leidel BA, Kirchhoff C, Bogner V, Braunstein V, Biberthaler P, Kanz K-G. 2012. Comparison of intraosseous versus central venous vascular access in adults under resuscitation in the emergency department with inaccessible peripheral veins. Resuscitation 83:40–45.

Leidel BA, Kirchhoff C, Bogner V, Stegmaier J, Mutschler W, Kanz K-G, Braunstein V. 2009. Is the intraosseous access route fast and efficacious compared to conventional central venous catheterization in adult patients under resuscitation in the emergency department? A prospective observational pilot study. Patient Safety in Surgery 3:24.

Luck RP, Haines C, Mull CC. 2010. Intraosseous Access. The Journal of Emergency Medicine 39:468–475.

Macnab A, Christenson J, Findlay J, Horwood B, Johnson D, Jones L, Phillips K, Pollack C, Robinson D, Rumball C, et al. 2000. A New System for Sternal Intraosseous Infusion in Adults. Prehospital Emergency Care 4:173–177.

McCarthy G, O'Donnell C, O'Brien M. 2003. Successful intraosseous infusion in the critically ill patient does not require a medullary cavity. Resuscitation 56:183–186.

Minville V, Pianezza A, Asehnoune K, Cabardis S, Smail N. 2006. Prehospital intravenous line placement assessment in the French emergency system: a prospective study. European Journal of Anaesthesiology 23:594–597.

Orlowski JP. 1984. My kingdom for an intravenous line. Am. J. Dis. Child. 138:803.

Orlowski JP. 1994. Emergency alternatives to intravenous access. Intraosseous, intratracheal, sublingual, and other-site drug administration. Pediatr. Clin. North Am. 41:1183–1199.

Paxton JH. 2012. Intraosseous vascular access: A review. Trauma 14:195–232.

Paxton JH, Knuth TE, Klausner HA. 2009. Proximal Humerus Intraosseous Infusion: A Preferred Emergency Venous Access: The Journal of Trauma: Injury, Infection, and Critical Care 67:606–611.

Peutrell JM. 2006. Intraosseous cannulation. Anaesthesia & Intensive Care Medicine 7:28–30.

Prentice AM, Jebb SA. 2001. Beyond body mass index. Obesity Reviews 2:141–147.

Reades R, Studnek J R, Garrett J S, Vandeventer S, Blackwell T. 2011. Comparison of first-attempt success between tibial and humeral intraosseous insertions during out-of-hospital cardiac arrest. Prehospital Emergency Care 15:278–281.

Reades R, Studnek JR, Vandeventer S, Garrett J. 2011a. Intraosseous Versus Intravenous Vascular Access During Out-of-Hospital Cardiac Arrest: A Randomized Controlled Trial. Annals of Emergency Medicine 58:509–516.

Rivera AM, Strauss KW, van Zundert A, Mortier E. 2005. The history of peripheral intravenous catheters : How little plastic tubes revolutionized medicine. Acta anaesthesiologica belgica 56:271–282.

Rosenberg H, Cheung WJ. 2013. Intraosseous access. CMAJ 185:E238.

Sardinha LB, Going SB, Teixeira PJ, Lohman TG. 1999. Receiver operating characteristic analysis of body mass index, triceps skinfold thickness, and arm girth for obesity screening in children and adolescents. Am. J. Clin. Nutr. 70:1090–1095.

Standring S. 2008. Gray's Anatomy : Gray's Anatomy : The Anatomical Basis of Clinical Practice (40th Edition). Jordon Hill, GBR: Churchill Livingstone.

Tarrow CAB, Turkel H, Thompson CMS. 1952. INFUSIONS VIA THE BONE MARROW AND BIOPSY OF THE BONE AND BONE MARROW. Anesthesiology 13:501–509–501–509.

Teleflex Incorporated. 2015. EZIO-Family_01-text.jpg (JPEG Image, 340 × 300 pixels) - Scaled (0%). [accessed 2014 Apr 9]. http://www.teleflex.com/en/usa/images/ems/EZIO-Family_01-text.jpg

The Science and Fundamentals of Intraosseous Vascular Access. 2013. Second Edition. Shavano Park (TX): Vidicare Corporation. Available from http://www.teleflex.com/en/usa/ezioeducation/documents/EZ-IO_SAFIOVA-M-607%20Rev%20B-PrintVersion.pdf

Tocantins LM. 1940. Rapid Absorption of Substances Injected into the Bone Marrow. Exp Biol Med (Maywood) 45:292–296.

Tocantins LM, O'neill JF. 1945. Complications of Intra-Osseous Therapy. Ann. Surg. 122:266–277.

Tocantins LM, O'Neill JF, Jones HW. 1941. Infusions of blood and other fluids via the bone marrow: application in pediatrics. JAMA 117:1229–1234.

Tocanttns LM, O'Neill JF. 1940. Infusion of Blood and Other Fluids into the Circulation via the Bone Marrow. Exp Biol Med (Maywood) 45:782–783.

Waisman M, Waisman D. 1997. Bone marrow infusion in adults. International Journal of Trauma Nursing 3:103.

Waismed Ltd. 2009. adultbig.png (PNG Image, 240 × 180 pixels) - Scaled (0%). [accessed 2014 Apr 9]. http://www.waismed.com/Pics/adultbig.png

Warren D, Kissoon N, Sommerauer J, Rieder M. 1993. Comparison of Fluid Infusion Rates Among Peripheral Intravenous and Humerus, Femur, Malleolus, and Tibial Intraosseous Sites in Normovolemic and Hypovolemic Piglets. Annals of Emergency Medicine 22:183–186.

Weiser G, Hoffmann Y, Galbraith R, Shavit I. 2012. Current advances in intraosseous infusion – A systematic review. Resuscitation 83:20–26.

Wellens RI, Roche AF, Khamis HJ, Jackson AS, Pollock ML, Siervogel RM. 1996. Relationships between the Body Mass Index and body composition. Obes. Res. 4:35–44.